19th Australasian Fluid Mechanics Conference
Melbourne, Australia
8-11 December 2014

Experimental Investigation of Wall-mounted Finite Airfoil Flow Noise

D. J. Moreau[1], C. J. Doolan[1], W. N. Alexander[2], T. W. Meyers[2] and W. J. Devenport[2]

[1]School of Mechanical Engineering
The University of Adelaide, Adelaide, SA 5005, Australia

[2]Aerospace and Ocean Engineering
Virginia Tech, Blacksburg, VA 24061, USA

Abstract

This paper presents a recent experimental program that measures the flow-induced noise generated by a wall-mounted finite airfoil in the Stability Wind Tunnel at Virginia Tech, USA. Far-field noise measurements have been taken at a single observer location and with a microphone array at a Reynolds number of $Re_c = 1.6 \times 10^6$ (based on airfoil chord) and for a variety of airfoil angles of attack from $\alpha = 0^\circ$ to 8°. The experimental data presented in this paper give insight into the affect of three-dimensionality on noise generation and show how flow at the junction and tip influence noise production at the source locations.

Introduction

The noise produced by flow interaction with a wall-mounted finite airfoil is important for a range of applications including submarine hydrofoils mounted to a hull, wind turbine blades mounted to a hub or the stators in an aeroengine that are connected to an outer wall. There is however, limited experimental data available on this topic as most previous studies on airfoil noise focus on two-dimensional or semi-infinite airfoil models [2–4, 8–10]. Compared to its two-dimensional counterpart, the flow around a wall-mounted finite airfoil is much more complicated as it is three-dimensional, with boundary layer impingement at the airfoil-wall junction and flow over the airfoil tip, as shown in figure 1. In the lower boundary layer, a horseshoe vortex system is present around the airfoil base and extends into the wake [6]. Vortex structures may also form at the tip of the finite airfoil, convect downstream of the airfoil trailing edge and eventually form a trailing vortex [7]. These flow features affect noise production in ways that are not yet fully understood and this is therefore the focus of the present study.

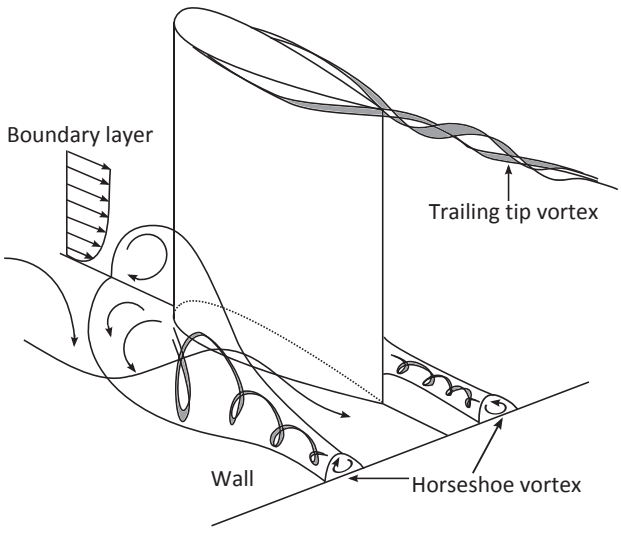

Figure 1. Flow structure of a wall-mounted finite airfoil.

This paper presents a novel wall-mounted finite airfoil flow-induced noise experiment conducted in the Virginia Tech Stability Wind Tunnel. Acoustic test data taken with a single microphone and a microphone array are presented at a high Reynolds number of $Re_c = 1.6 \times 10^6$ and for a range of airfoil angles of attack from $\alpha = 0^\circ$ to 8° to show the influence of tip flow, boundary layer impingement and three-dimensionality on noise production.

Experimental Method

Experimental Facility

Experiments were performed in the Stability Wind Tunnel at Virginia Tech as shown in figure 2. This facility has low turbulence levels of up to 0.03% and can achieve flow speeds of up to 80 m/s depending on blockage. The Stability Wind Tunnel has interchangeable aerodynamic and anechoic test sections that have dimensions of 1.83 m $\times$ 1.83 m $\times$ 7.3 m. In this study, measurements were taken in the anechoic test section [5] as shown in figure 2 (b). This test section has tensioned Kevlar walls that contain the flow while being acoustically transparent. Sound generated in the test section passes through the Kevlar walls into two anechoic chambers located on either side of the test section where acoustic instrumentation can be placed. The chambers have dimensions of 5.6 m $\times$ 2.8 m $\times$ 4.2 m and are lined with 0.61 m high foam wedges to dampen acoustic reflections. The ceiling and floor of the anechoic test section are formed from a series of perforated metal panels that are covered with Kevlar cloth. The volume behind these panels is filled with 0.46 m high foam wedges to further eliminate acoustic reflections.

Test Model

The test model consisted of a finite length NACA 0012 airfoil with flat ended tip. The airfoil has a chord of $C = 0.4$ m, a span of $L = 1.2$ m and an aspect ratio of $L/C = 3$, corresponding to a length to thickness ratio of $L/T = 25$. As shown in figure 3, the airfoil was flush mounted to the wind tunnel ceiling so that the airfoil length axis (span) was perpendicular to the direction of the flow. The leading edge of the airfoil was positioned at 3.43 m downstream of the test section entrance. In this study, the Kevlar covered perforated panels located on the ceiling upstream of the test model were replaced with solid metal ones to ensure high quality boundary layer flow at the airfoil-wall junction. In all tests, the airfoil was untripped, allowing natural boundary layer transition to occur. Measurements were taken for an airfoil angle of attack of $\alpha = 0^\circ$ to 8°.

Measurement Equipment and Procedure

Experiments were conducted at a free-stream velocity of $U_\infty =$ 60 m/s corresponding to Reynolds numbers based on airfoil chord of $Re_c = 1.6 \times 10^6$.

Noise data were measured at a single observer location using a

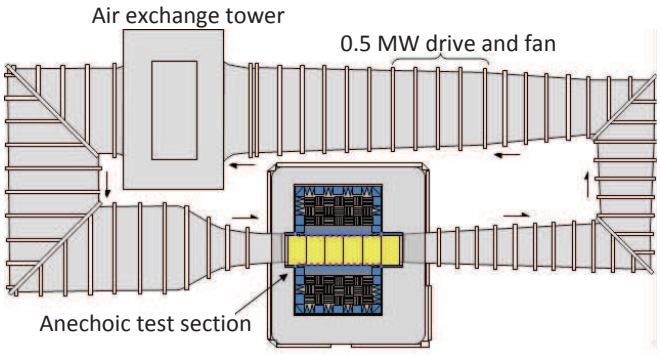

(a) Top view of the Stability Wind Tunnel. Adapted from [1].

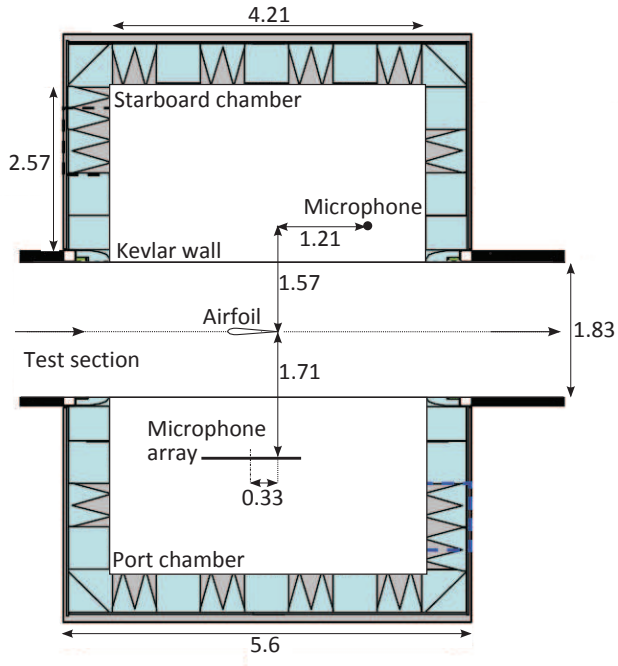

(b) Top view of the anechoic test section. Adapted from [5].

Figure 2. The Stability Wind Tunnel. Dimensions in m.

B&K 4190 1/2" microphone located in the starboard anechoic chamber. The microphone was held in a stand at a height of 0.81 above the test section floor. The position of the microphone relative to the airfoil is shown in figure 2(b). Acoustic data were recorded with B&K Pulse 14 software and a 3050-A LXI data acquisition system at a sampling frequency of 2^{16} Hz for a sample time of 32 s.

An AVEC microphone array located in the port anechoic chamber was also used to measure the sound emitted by the wall-mounted finite airfoil. The array has an outer diameter of 1.1 m and its centre was positioned 0.93 m above the test section floor. The location of the microphone array relative to the airfoil is shown in figure 2(b). The array consists of 117 Panasonic model WM-64PNT Electret microphones arranged in a 9-armed spiral. The 117 microphones were connected to an AVEC designed signal conditioning and filtering box and two 64-channel PCI-based data acquisition cards. Data from the 117 microphones were acquired at a sampling frequency of 51,200 Hz for a sample time of 32 s. Custom-designed beamforming software was used to collect the data as well as for analysis. Each of

Figure 3. The wall-mounted finite airfoil model in the Stability Wind Tunnel anechoic test section.

the microphone signals were transformed using a Fast Fourier Transformation with 200 blocks of 8192 samples per block. Maps of local sound pressure contributions (or sound maps) were obtained using AVEC's post-processing algorithm and are displayed in 1/12th octave bands.

Incoming Boundary Layer

To characterize the incoming flow conditions, the boundary layer profile on the ceiling of the test section at a location of 130 mm upstream of the airfoil leading edge location (but with the airfoil removed) was measured at $U_\infty = 60$ m/s using hot-wire anemometry. An Auspex single-wire probe with a wire length of 1 mm and a wire diameter of 5 μm was used. The sensor was operated using a Dantec Streamline anemometer, the output of which was recorded using an Agilent E1432 16-bit digitizer and positioned using a PD90x controller traverse. At each measurement location, hot-wire data were acquired at a sampling frequency of 25,600 Hz for a sample time of 13 s.

Figure 4 shows the incoming boundary layer profile plotted using inner variables. The boundary layer profile has the form of a fully developed zero pressure gradient boundary layer and has a semi-logarithmic region that compares well to the law of the wall profile using a von Karman constant of 0.41 and an offset of 5.2. The boundary layer thickness was measured to be $\delta = 68$ mm and therefore the incoming boundary layer height to airfoil span is $\delta/L = 0.057$.

Experimental Results

Figure 5 shows the acoustic spectra measured with the single microphone for the wall-mounted finite airfoil at $U_\infty = 60$ m/s and $\alpha = 0^\circ$ to 8°. The wind tunnel background noise measurement without the airfoil present is also shown for comparison.

At low angles of attack of $\alpha = 0^\circ$ and 2°, the airfoil noise levels are low and only sit above the background noise at frequencies below 1 kHz and between 2 and 4 kHz. A broad peak is observed in the noise spectra at a frequency of 3 kHz and this is attributed to vortex shedding from the trailing edge due to bluntness effects. When the angle of attack is increased to $\alpha = 4^\circ$,

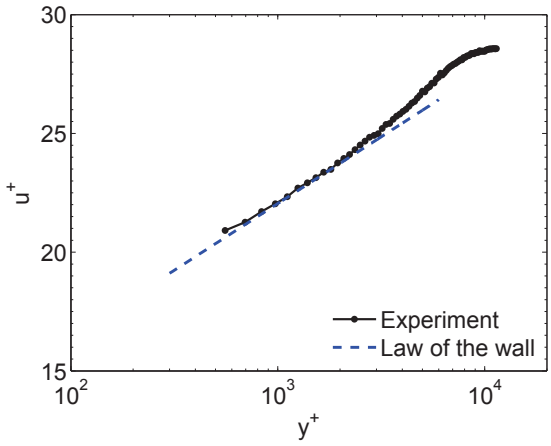

Figure 4. Incoming boundary layer profile in wall coordinates.

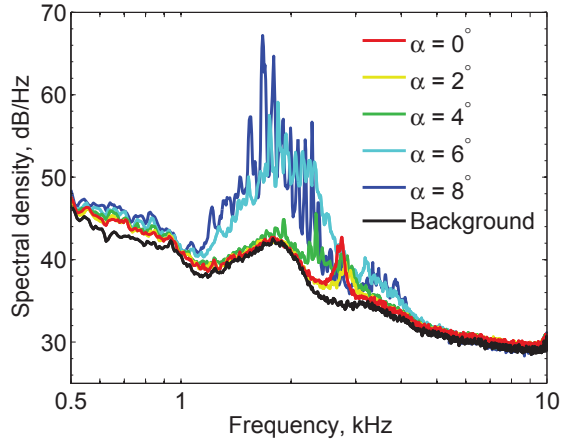

Figure 5. Acoustic spectra for the wall-mounted finite airfoil at $\alpha = 0^\circ$ to 8°.

the noise levels below 4 kHz are observed to increase slightly. Further increasing the angle of attack to $\alpha = 6^\circ$ results in a number of high amplitude tones being visible in the noise spectrum. At $\alpha = 6^\circ$ and 8°, the noise radiated by the wall-mounted finite airfoil consists of a broadband contribution and a number of discrete equispaced tones. The Strouhal number based on airfoil thickness, T, of the difference between two consecutive discrete tonal frequencies is $St_T = 0.072$ and 0.096 at $\alpha = 6^\circ$ and 8°, respectively.

The tonal noise produced by the wall-mounted finite airfoil at high angles of attack of $\alpha = 6^\circ$ and 8° in figure 5 is attributed to the presence of laminar-transitional flow over (at least one side of) the airfoil. Studies on two-dimensional airfoil noise have similarly reported the production of acoustic tones in the presence of laminar-transitional boundary layer flow with tonal noise production often being associated with an aeroacoustic feedback loop between instabilities in the laminar-transitional boundary layer and acoustic waves at the trailing edge. Lowson et al. [8] developed a tonal envelope that defines the angles of attack and Reynolds numbers for which tones are expected to occur due to an aeroacoustic feedback mechanism as shown in figure 6. This tonal envelope was derived from experimental data sets for two-dimensional NACA 0012 airfoils [10, 8]. Figure 6 shows that at high Reynolds numbers, tonal noise production can only be expected to occur at high angles of attack as the pressure surface boundary layer will only remain laminar-transitional to the trailing edge under these conditions. The operating conditions for which tones are produced by the wall-mounted finite airfoil just fall within the predicted tonal envelope. This suggests that tonal noise generation is occurring presumably in the same manner as in other studies on two-dimensional airfoils.

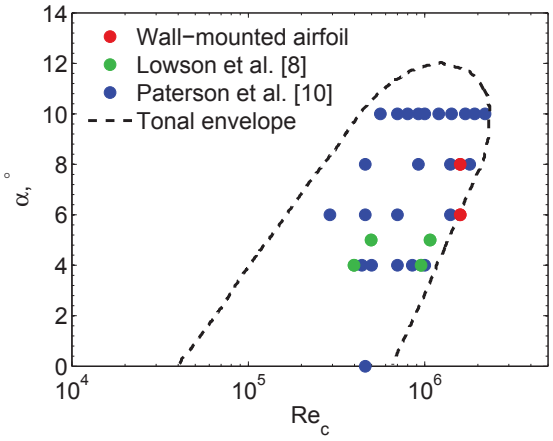

Figure 6. Tonal envelope predicting the operating conditions for tonal noise production from a NACA 0012 airfoil.

Figure 7 shows sound maps taken with the microphone array for the wall-mounted finite airfoil at $U_\infty = 60$ m/s and $\alpha = 0^\circ$. In this figure, x is the streamwise direction where the flow is from left to right and y is the spanwise direction. A position of $x = 0$, $y = 0$ corresponds to the centre of the test section. The sound maps are presented at 1/12th octave band centre frequencies of 1 to 4.5 kHz and the location of the airfoil is shown in white.

Figure 7(a) shows that at a frequency of 1 kHz, the noise source appears primarily at the airfoil leading edge-wall junction. The dominant noise source then shifts to the airfoil trailing edge-wall junction at a frequency of 2 kHz (see figure 7(b)). Despite the boundary layer height being only 6% of the airfoil span, junction noise is the dominant generation mechanism at frequencies of 1 to 2 kHz. Figure 7(c) shows that at a frequency of 3 kHz, airfoil trailing edge noise is the primary noise generation mechanism. This agrees with the noise spectrum of figure 5 which displays a broad peak at 3 kHz attributed to trailing edge vortex shedding noise due to bluntness effects. At higher frequencies of 3.55 and 4.5 kHz the trailing edge tip is the dominant noise source. An additional noise source is also detected at the airfoil trailing edge - wall junction at a frequency of 4.5 kHz.

Conclusions

This paper has presented an experimental investigation on the noise generated by a wall-mounted finite airfoil at high Reynolds number. The results have included far-field acoustic spectra measured at a range of airfoil angles of attack and sound maps taken with a microphone array. Angle of attack has been shown to significantly effect the spectral content of sound radiated by the wall-mounted finite airfoil and to influence whether tonal noise production occurs as well as the magnitude and frequency of any tonal noise components. The beamforming sound maps have shown that at zero angle of attack, junction noise dominates at low frequencies below 2 kHz. The airfoil trailing edge becomes the dominant noise source at a frequency of 3 kHz and then tip noise is the primary noise generation mechanism at high frequencies of 3.55 kHz and above.

It is worth noting that this experimental investigation is part of an ongoing study to obtain a comprehensive database of experimental flow and far-field noise data for a wall-mounted finite airfoil. The experimental database will be used to provide insight into how tip flow, boundary layer impingement and three-dimensionality affect airfoil noise production.

Acknowledgements

This work has been supported by the Australian Research Council under linkage grant LP110100033 'Understanding and predicting submarine hydrofoil noise', the Australian-American Fulbright Commission, the Sir Ross and Sir Keith Smith Fund and the South Australian Premier's Research and Industry Fund Catalyst Research Grant Program. In addition, the authors would like to thank Bill Oejtens, Dr Aurelien Borgoltz and Dr Nanya Intaratep for their valuable assistance during the experimental test campaign.

References

[1] Alexander, W.N., Devenport, W., Morton, M.A. and Glegg, S.A.L., Noise from a rotor ingesting a planar turbulent boundary layer, *19th AIAA/CEAS Aeroacoustics Conference*, AIAA 2013 – 2285, Berlin, Germany, 2013.

[2] Blake, W.K., *Mechanics of Flow Induced Sound and Vibration*, volume II: Complex flow-structure interactions, Academic Press, New York, 1986.

[3] Brooks, T.F. and Hodgson, T.H., Trailing edge noise prediction from measured surface pressures, *Journal of Sound and Vibration*, **78**(1), 1981, 69 – 117.

[4] Brooks, T.F., Pope, D.S. and Marcolini, M. A., Airfoil self-noise and prediction, NASA Reference Publication 1218, 1989.

[5] Devenport, W.J., Burdisso, R.A., Borgoltz, A., Ravetta, P.A., Barone, M.F., Brown, K.A. and Morton, M.A., The Kevlar-walled anechoic wind tunnel, *Journal of Sound and Vibration*, **332**, 2013, 3971–3991.

[6] Devenport, W.J. and Simpson, R.L., Time-dependent and time-averaged turbulence structure near the nose of a wing-body junction, *Journal of Fluid Mechanics*, **210**, 1990, 23 – 55.

[7] Giuni, M. and Green, R.B., Vortex formation on squared and rounded tip, *Aerospace Science and Technology*, **29**, 2013, 191 – 199.

[8] Lowson, M.V., Fiddes, S.P. and Nash, E.C., Laminar boundary layer aeroacoustic instabilities, *32nd Aerospace Sciences Meeting*, AIAA 94 0358, Reno, NV, 1994.

[9] Moreau, D.J., Brooks, L.A. and Doolan, C.J., The effect of boundary layer type on trailing edge noise from sharp-edged flat plates at low-to-moderate Reynolds number, *Journal of Sound and Vibration*, **331**(17), 2012, 3976 – 3988.

[10] Paterson, R.W., Vogt, P.G., Fink, M.R and Munch, C.L., Vortex noise of isolated airfoils, *Journal of Aircraft*, **10**(5), 1973, 296 – 302.

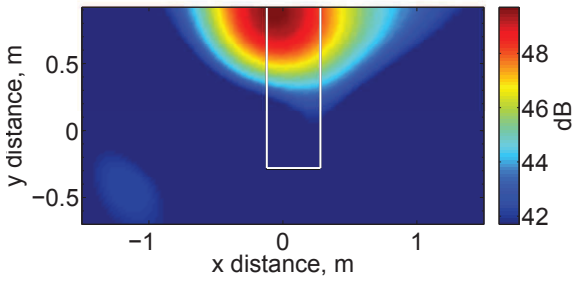

(a) $f = 1$ kHz.

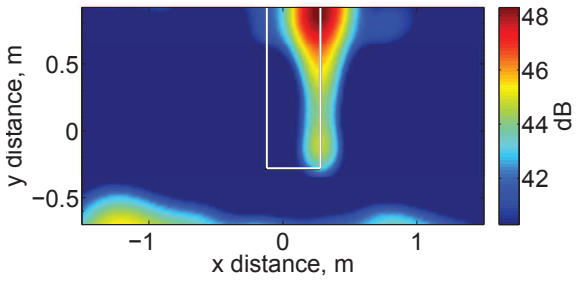

(b) $f = 2$ kHz.

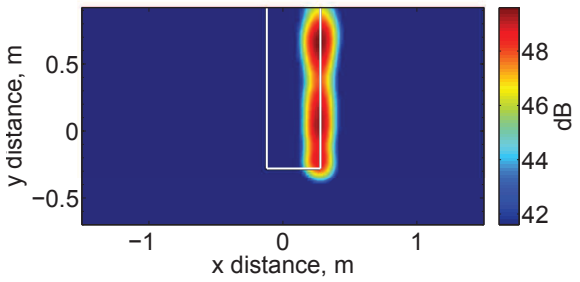

(c) $f = 3$ kHz.

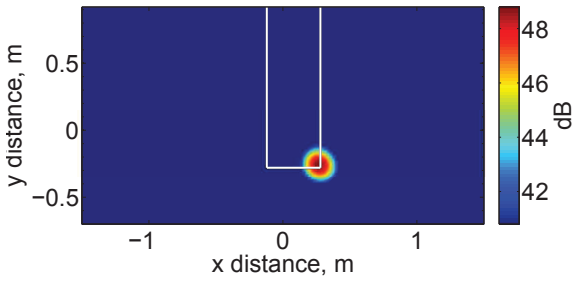

(d) $f = 3.55$ kHz.

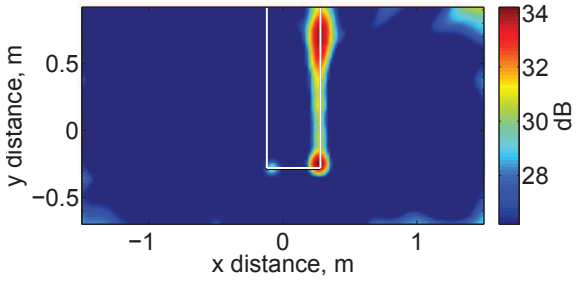

(e) $f = 4.5$ kHz.

Figure 7. Sound maps for the wall-mounted finite airfoil at $\alpha = 0°$.